COMMUNICATIONS IN INFORMATION AND SYSTEMS
Vol. 4, No. 2, pp. 165-180, March 2005

003

SURFACE SEGMENTATION USING GLOBAL CONFORMAL STRUCTURE*

YALIN WANG†, XIANFENG GU‡, AND SHING-TUNG YAU§

Abstract. Surface segmentation is a fundamental problem in computer graphics. It has various applications such as metamorphosis, surface matching, surface compression, 3D shape retrieval, texture mapping, etc. All orientable surfaces are Riemann surfaces, and admit conformal structures. This paper introduces a novel surface segmentation algorithm based on its conformal structure. Each segment can be conformally mapped to a planar rectangle, and the transition maps are planar translations. The segmentation is intrinsic to the surface, independent of the embedding, and consistent for surfaces with similar geometries. By using segmentation based on conformal structure, the mapping between surfaces with arbitrary topologies can be constructed explicitly. The method is rigorous, efficient and automatic. The segmentation can be applied to surface morphing, construct conformal geometry image, convert mesh to Spline surface, solve Partial Differential Equations on arbitrary surfaces, etc.

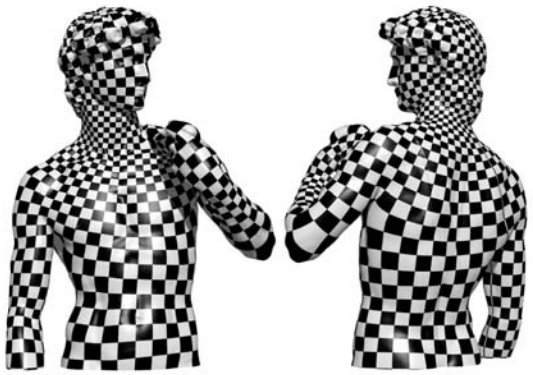

1. Introduction. Surface segmentation is a technique which decomposes a surface mesh into various sub-meshes. Similar to image segmentation [SM00] in image processing, one can simplify some problems by surface segmentation. For example, for texture mapping, it is a standard practice to decompose the surface into several parts, make texture mapping on each part and merge them to get the final result of the texture mapping [LPRM02]. Surface segmentation benefits various applications, such as metamorphosis [GSL*99, STK02], surface simplification [GWH01], collision detection [LTTH01], control-skeleton extraction [KT03], and surface matching, etc.

All oriented metric surfaces are Riemann surfaces, and they admit global conformal parameterization. The global conformal parameterization is such a geometric construction that can satisfy the segmentation and parameterization requirements. Conformal surface parameterizations have many merits, such as preserving angular structure, being intrinsic

*Received on May 15, 2004; accepted for publication on November 15, 2004.
†Department of Mathematics, UCLA, Los Angeles, CA 90095. E-mail: ylwang@math.ucla.edu
‡Computer Science Department, State University of New York at Stony Brook, Stony Brook, New York 11794-4400. E-mail: gu@cs.sunysb.edu
§Department of Mathematics, Harvard University, Cambridge, MA 02138. E-mail: yau@math.harvard.edu

to geometry, stable with respect to different triangulations and small deformations. It has been widely used for many applications, such as non-distorted texture mapping [LPRM02], [HAT*00b],[KSG03], surface remeshing [AMD02b], surface fairing [L ́03], surface matching [GY02], brain mapping [AHTK99], [GWC*04] etc.

In this paper we propose a novel surface segmentation algorithm based on global conformal structure. There are finite zero points on the global conformal parameterization on a surface. Our algorithm automatically locate these zero points and trace the *horizontal and vertical trajectories* (roughly iso-parametric curves, details in 2) through zero points, then partition the surface to segments, such that each segment can be conformally mapped to a parallelogram on the *uv* plane. The conformality is also preserved along the boundaries. We call this kind of segmentation **holomorphic flow segmentation**. We further demonstrate our algorithm by applying it on metamorphasis and surface matching problems.

The pictures on the beginning of the paper illustrate some experimental results of our algorithm. The first two figures show the global conformal parameterization of Michelangelo's David surface. The second two figures show the result segments both in $\mathbb{R}$ and the parameterization domain, separately. The surface segments are color encoded, and conformally mapped onto rectangles on the parameter plane.

1.1. Contributions. This paper introduces algorithms to compute surface segmentation using conformal structure. The method is based on Riemann surface theories and differential geometry, therefore it is rigorous and general. The method has the following metrics,

1. The algorithm is intrinsic and independent of surface embedding. Because conformal structure is determined by the metric, not the embedding, isometric surfaces will have the same holormorphic segmentations. For example, the human body surfaces with different postures can be roughly treated as isometric surfaces, and they can be segmented consistently. This is valuable for animation purpose.
2. The algorithm is stable with respect to small deformations of the geometry. The computation of conformal structure is equivalent to solve elliptic partial differential equations on the surface, whose solutions continuously depend on the geometries.

So our method is insensitive to the noise of the geometric information, consistent with different resolutions.

3. The algorithm is general for surfaces with arbitrary topologies, especially good for surfaces with higher genus.

The segmented results are very useful for further applications. For example, by this method, 3D metamorphsis can be converted to 2D metamorphsis on rectangles.

Furthermore, with conformal parameterization, only two functions, *conformal factor* and *mean curvature*, are enough to represent a surface [Jos91]. With our holomorphic flow segmentation, one can represent each segment using these two functions defined on the conformal parameter domain. This representation is invariant under rigid motion of the surface and convenient for surface matching. We define surface distance metric based on this unique representation.

1.2. Previous Works. Different surface segmentation approaches have been studied in the past. Chazelle et al. [CP97, CDST97] present convex decomposition schemes. However, small concavities in the objects result in over-segmentation. In [MW99] a watershed decomposition is described. A post-processing step resolves over-segmentation. One problem with the algorithm is the dependency on the exact triangulation of the model. In [GWH01], face clustering is proposed so that the cluster may be well approximated with planar elements. Li et al. [LTTH01] used skeletonization and space sweep. However, smoothing effects might cause the disappearance of features for which it is impossible to get a decomposition. Shlafman et al. [STK02] proposed a K-means based clustering algorithm. The meaningful components of the objects are found. However, the boundaries between the patches are often jagged and not always correct. Katz and Tal [KT03] introduced a method using fuzzy clustering and cuts. It computes a decomposition into the meaningful components of a given mesh and avoids over-segmentation and jaggy boundaries between the components. The drawback of this method is that the boundaries between different components depend on the surface embedding and not intrinsic to the surface geometry. The same geometric surface may get different segmentation results due to different embedding.

Surface parameterization has been studied extensively in the graphics field. Most works in conformal parametrization only deal with genus zero surfaces. Eck et al. [EDD*95] introduce the *discrete harmonic map*, which approximates the continuous harmonic maps by minimizing a *metric dispersion* criterion. Floater introduces *shape-preserving* method in [Flo97]. Then the method is improved in [Flo03] using *mean value coordinates*. Hormann and Greiner [HG99] measure the conformality in a different way using *most isometric parameterizations* method. Haker et al. [HAT*00a] introduce a method to compute a global conformal mapping from a genus zero surface to a sphere by representing the Laplacian-Beltrami operator as a linear system. Alliez et al. [AMD02a] compute the discrete Dirichlet energy and apply conformal parametrization to interactive geometry remeshing. Lévy et al. [LPRM02] compute a quasi-conformal parametrization by approximating the Cauchy-Riemann equation

using the least squares method. For surfaces with arbitrary topologies, Gu and Yau [GY02] introduces a general method for global conformal parameterizations based on the structure of the cohomology group of holomorphic one-forms. They generalize the method for surfaces with boundaries in [GY03].

2. Theoretic Background. The holomorphic segmentation is based on the fact that all oriented metric surfaces are Riemann surfaces and admit conformal structures. Therefore they have global conformal parameterizations. By tracing special curves induced by the global conformal parameterization, the surfaces can be canonically segmented. Because the segmentation depends on the conformal structure only, isometric surfaces have the same segmentations.

Riemann Surface and Global Conformal Parameterization

A *Riemann surface* is a connected Hausdorff topological surface S with a family of open coverings $\{U_\alpha\}$ and a family of mappings $z_\alpha : U_\alpha \to \mathbb{C}$, satisfying the following conditions:

- $z_\alpha : U_\alpha \to \mathbb{C}$ is a homeomorphism to an open set $z_\alpha(U_\alpha)$ in C.
- if $U_\alpha \cap U_\beta \neq \phi$, function

$$z_\beta \circ z_\alpha^{-1} : z_\alpha(U_\alpha \cap U_\beta) \to z_\beta(U_\alpha \cap U_\beta) \tag{1}$$

  is holomorphic and the inverse is also holomorphic. (U_α, z_α) is a local holomorphic coordinates.

Namely, a holomorphic coordinate is a **local conformal parameterization** and the first fundamental form can be written as

$$ds^2 = \lambda(z) dz d\bar{z} \tag{2}$$

(equivalently $\lambda(u,v)(du^2 + dv^2)$), where $\lambda(z) > 0$ is the stretching factor, and called **conformal factor**.

A **global conformal parameterization** of surface S is a parameterization $\phi : S \to \mathbb{C}$, such that equation 2 holds everywhere and there might be several exceptional points. The complex derivative of a global conformal parameterization is called a **holomorphic 1-form**. At each local holomorphic coordinate chart, the holomorphic 1-form can be formulated as $\omega = f(z)dz$, where $f(z)$ is a holomorphic function. At the exceptional points, $f(z)$ equals to zero, and these points are called **zero points**. For genus $g \geq 1$ surface, there will be $2g-2$ zero points.

Horizontal Trajectory and Vertical Trajectory

A holomorphic 1-form ω can induce a *quadratic differential form*, ω^2. A **vertical trajectory** c of ω is a curve, such that such that along c $\omega^2 < 0$. A *horizontal trajectory* c of ω is a curve, such that such that along c $\omega^2 > 0$. The horizontal and vertical trajectories through zero points will be used to segment the surface.

Structure of Holomorphic Flow Segmentation

Let S be a compact Riemann surface and ω a holomorphic 1-form on S. Each horizontal or vertical trajectory is a union of closed loops. The horizontal and vertical trajectories

through zero points can segment the surface to topological disks, each disk can be conformally mapped to a parallelogram on the plane. The conformal mapping can be obtained by integrating ω on the patch.

For the case of a torus, there is no zero point on a holomorphic 1-form. The whole torus will be conformally mapped to one parallelogram on the complex plane.

The holomorphic flow segmentation induces a complex $G = \{V, E, F\}$, where V are zero points, E are horizontal and vertical trajectories, F are segments. We call G as **holomorphic flow complex**.

Symmetric Surface

For special *symmetric* surfaces (by symmetry, we mean the canonical period matrix has zero imaginary part [Jos91]), each segment can be conformally mapped to a rectangle.

In our experiments, we perform topology modification first on genus zero closed surface in order to improve the quality of their global conformal parameterization, as explained in [GY02]. Then we *double cover* the open surface to a closed symmetric one. The following is the method for double covering, first we get two copies of the same open surface, reverse the orientation of one of them, and glue two copies along their boundaries.

If the surface is symmetric, the horizontal and vertical trajectories are iso-parametric curves. For asymmetric surfaces, the algorithms are very similar with extra affine mappings to covert each parallelogram on the parameter plane to rectangles. In the following discussion, we always assume the surface is symmetric and use vertical trajectory and iso-u curve, horizontal trajectory and iso-v curve interchangably.

3. Algorithms for Holomorphic Flow Segmentation. We use triangular meshes to approximate surfaces. Suppose K is a simplicial complex, and a mapping $r : |K| \to \mathbb{R}^3$ embeds $|K|$ in $\mathbb{R}^3$. Then (K, r) is called a *triangular mesh*. The sets K_n, where $n = 0, 1, 2$, are the $n-$*simplicies* (sets of vertices, edges, and faces, respectively). The holomorphic 1-form ω can be represented as a function $\omega : K_1 \to \mathbb{R}^2$.

The algorithm for computing Riemann surface structure of a mesh is equivalent to computing a holomorphic 1-form basis. The major steps for computing the complete conformal parameterization atlas are as follows:

1. Modify the topology of the surface (cut the mesh) in order to improve the quality of the parameterization.
2. Compute a fundamental domain $\bar{S}$ from mesh S.
3. Compute a homology basis from the boundary of the fundamental domain $\bar{S}$.
4. Compute a holomorphic 1-form basis from the homology basis.
5. Select a holomorphic 1-form ω, and integrate ω on $\bar{S}$ to get a global conformal parameterization ϕ.
6. Locate zero points of ω using ϕ.
7. Trace horizontal and vertical trajectories through the zero points using ϕ.
8. Segment S by the horizontal and vertical trajectories, using ϕ to map each segment

conformally to a rectangle on the plane.

Steps 1-5 compute the global conformal parameterization of the surface. However, the segments obtained in step 8 may have the images of zero points on the plane. As shown in Figure 1, the zero points of a parameterization are singularities, or points whose neighborhood on the surface has a special configuration when mapped to the plane. The details for computing steps 1-5 and 8 have been thoroughly explained in [GY02], [GY03] and [GWY04]. This work will focus on steps 6 and 7, namely, locating the zero points of a holomorphic 1-form and tracing the horizontal and vertical trajectories.

Tracing Vertical Trajectories

Given any u-value u_0, we want to trace the vertical trajectories on the surface S. First, we compute the fundamental domain $\bar{S}$ of S, the holomorphic 1-form ω, and the conformal map ϕ. The algorithm proceeds as follows:

1. Map $\bar{S}$ to the plane using ϕ; $\phi(\bar{S})$ are planar regions.
2. For the chosen parameter u-value u_0 (see "Locating Zero Points", below), slice $\phi(\bar{S})$ along the line $u = u_0$.
3. When, or if, the curve ends at a boundary on $\bar{S}$, its connecting curve on $\bar{S}$ will continue along another u-value u_1 on the plane. The intersection point p_i on $\bar{S}$ between the vertical trajectories and the boundary maps to two points, one of which we have just encountered at u-value u_0, and its dual boundary point, which has a different u-value, u_1. Locate this point on the plane.
4. Continue slicing $\bar{S}$ along the vertical trajectory $u = u_1$ until we reach the next boundary point, whose dual point has u-value is u_2. Find the dual point, and continue slicing $\bar{S}$ along the connecting curve.
5. Repeat this procedure (slice along u_i, find dual boundary point, slice along u_{i+1}) until all the traced curves, which are curved segments joined at the boundaries on $\bar{S}$, form a closed loop.

The horizontal trajectories can be traced in the similar way.

Locating Zero Points

Having found a holomorphic 1-form ω, and the fundamental domain $\bar{S}$, we can estimate the position of zero points on the mesh. The zero points have the following properties:

- The conformal factor $\lambda(u,v)$ is zero at zero points.
- The vertical trajectories only intersect at zero points.

Suppose a vertex v_0 has neighbors $v_1, v_2, \cdots, v_n$. First, we estimate the conformal factor for each vertex by the following formula:

$$\lambda(v_0) = \frac{1}{n}\sum_{i=1}^{n} \frac{|\omega([v_0, v_i])|^2}{|r(v_0) - r(v_i)|^2},$$

where $[v_0, v_i]$ represent the edge from v_0 to v_i. Then, we choose the vertices with local minimal λ as the candidates for zero points.

Next, we compute the vertical trajectories through the candidate vertices. By adjusting

the u value until the corresponding vertical trajectories intersects itself, we can locate the desired zero point, the intersection point of the curve. The configuration of an vertical trajectory in a neighborhood of a zero point can be classified by three types. Locally, it may look like one of three curves on the surface (using (u,v) for the local, planar neighborhood of a zero point): $uv = +1$, $uv = -1$, or $uv = 0$, which we label as types *I*, *II*, and *III* respectively (see Figure 1). We are looking for a type *III* vertical trajectory, which will intersect itself at the zero point. The following is the detailed algorithm to adjust u:

1. Compute the fundamental domain $\bar{S}$, compute the holomorphic 1-form ω, and compute the conformal mapping $\phi : \bar{S} \to \mathbb{C}$.
2. Compute the conformal factor for each vertex; use the vertices with minimal conformal factor as the candidates for the zero points.
3. Choose one candidate p, record its u-value u_0, and trace vertical trajectory with this u-value.
4. Randomly choose another u-value u_1 close to u_0 and trace the vertical trajectory for u_1 until it is of a different type than the vertical trajectory for u_0.
5. Perform a binary search on u in $[u_0, u_1]$, until the configuration of the vertical trajectories is of type *III*. Return the intersection point as the zero point.

If the resolution of the mesh is not high enough, it is possible that we can only get type *I* and *II* vertical trajectories. In this case, we can subdivide the neighborhood of the zero point and repeat the process.

4. Constrained Harmonic Map. Some researchers report their work on geometric morphing. Gregory et al. [GSL*99] and Alexa et al. [ACOL00] present morphing methods based on volumetric data while Ohtake et al. [OBA*03] and Praun et al. [PH03] propose morphing methods which rely on finding the point correspondence between surface vertices.

This section will explain how to match each pair of segments for two surfaces with consistent holomorphic flow segmentation. After segmentation, each segment has a conformal parameterization, each parameter domain is a parallelogram. By matching the parallograms by affine maps, the surfaces can be matched by the quasi-conformal maps directly. In applications, it is always desirable to match the sets of feature points. The constrained harmonic map will map the feature points and minize the stretching energy.

The basic pipe line is as follows: first we manually label the corresponding feature points; then we Delaunay triangulate the feature points on one segment, and induce the same triangulation for the second segment; by using a piecewise linear transformation, we find a initial homeomorphism between the segments; we then refine the mapping by minimizing the harmonic energy and finally to get a constrained harmonic map. After that, we can construct two geometry images with the same connectivity for the two segments, and build the morphing between them. The matching problem addressed here is similar to the one in [KSG03]. However, since we use global conformalization method, the geometric and parametric configuration of corresponding segments are very similar to each other. The process of computing

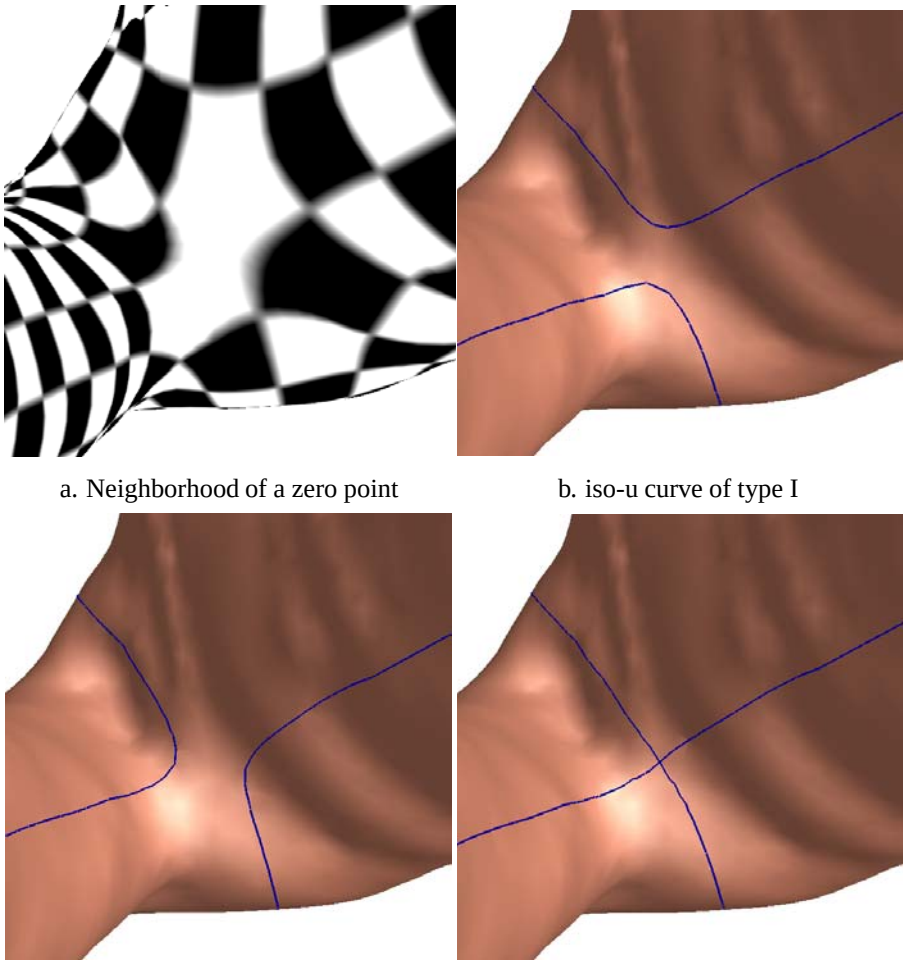

a. Neighborhood of a zero point b. iso-u curve of type I

c. iso-u curve of type II d. iso-u curve of type III

FIG. 1. *Algorithm for locating a zero point. The neighborhood of a zero point is shown in (a). The vertical trajectories (iso-u curves) have 3 types in the neighborhood. Type I is like the hyperbolic curve* $uv = +1$ *as shown in (b), type II* $uv = -1$ *in (c), and type III* $uv = 0$ *in (d). Suppose the u-value of the zero point is* u_0*, then type I is of* $u > u_0$*, type II is of* $u < u_0$*, by adjusting u-value, we can find type III iso-u curves, the zero point is the intersection of the iso-u curve of* u_0*.*

the constrained harmonic map is simplified, such as it is unnecessary to add Steiner vertices.

Suppose the two surface segments are S and $\tilde{S}$ represented as triangle meshes and we manually pick the feature points on them. The feature points are subset of vertices including the four corners of the rectangle on the parameter plane, the points with high Gaussian curvature, and the major geometric features. For the human face example, the feature points are the tip of the nose, center of the eyes, corner of the mouths and eyes, etc.

Suppose $F = \{v_1, v_2, \cdots, v_n\}$ are feature points of S, $\tilde{F} = \{\tilde{v}_1, \tilde{v}_2, \cdots, \tilde{v}_n\}$ are feature

points of $\tilde{S}$, we would like to find a smooth map $\phi : S \to \tilde{S}$, such that

$$\phi(v_j) = \tilde{v}_j, \phi(\partial S) = \partial \tilde{S},$$

i.e. ϕ maps feature points to feature points, and maps the boundary of S to that of $\tilde{S}$. In order to improve the smoothness, we require ϕ to be harmonic, $\Delta\phi = 0$, where Δ is the Laplace-Beltrami operator.

It is difficult to find ϕ directly, instead we can find a harmonic map between the parameter domain of S and that of $\tilde{S}$. Suppose the conformal parameterization of S is τ, conformal parameterization for $\tilde{S}$ is $\tilde{\tau}$, then $\tau(S)$ and $\tilde{\tau}(\tilde{S})$ are rectangles in R^2. We want to find a harmonic map $\mu : R^2 \to R^2$, such that

$$\mu \circ \tau(v_j) = \tilde{\tau}(\tilde{v}_j), \mu \circ \tau(\partial S) = \tilde{\tau}(\partial \tilde{S}), \Delta\mu = 0,$$

where Δ is the Laplace operator defined on the plane. Then the map ϕ can be obtained by the following commutative diagram,

(3)
$$\begin{array}{ccc} S & \xrightarrow{\phi} & \tilde{S} \\ {\scriptstyle\tau}\downarrow & & \downarrow{\scriptstyle\tilde{\tau}} \\ R^2 & \xrightarrow[\mu]{} & R^2 \end{array}$$

$\phi = \tilde{\tau}^{-1} \circ \mu \circ \tau$. Because both τ and $\tilde{\tau}$ are conformal, μ is harmonic, therefore ϕ is also harmonic.

The algorithms can be summarized as the following,

1. **Inital Piecewise linear Map** We Delaunay triangulate the feature points $F \subset \tau(S)$, and induce a triangulation on $\tilde{F} \subset \tilde{\tau}(\tilde{S})$. Then use piecewise linear map $\mu_0 : \tau(S) \to \tilde{\tau}(\tilde{S})$ as the initial map.
2. **Heat flow minimization** We minimize the harmonic energy of the map, using the following heat flow method:

   $$\frac{\partial \tau}{\partial t} = -\Delta\tau$$

   where Δ is the Laplace operator, until the Laplacian of interior vertices are zero. In implementation, we use the discrete Laplace operator defined in [AMD02b].
3. Morphing After geting the constrained harmonic map ϕ, we can construct a geometric morphing sequence by using the following formulae

   $$r(u,v,t) = f(u,v,t)r(u,v) + (1 - f(u,v,t))\tilde{r}(\phi(u,v)),$$

   where $f(u,v,t) \in [0,1]$ is a blending function depends on both time the parameter position.

In our implementation, we remesh both the segments of S and $\tilde{S}$ to be conformal geometry images to improve the efficiency.

5. Surface Distance Metric. We define a new metric to measure the distance between two surfaces based on their Riemann surface structure. Given two surfaces S and $\tilde{S}$, we choose appropriate holomorphic 1-forms, ω on S and $\tilde{\omega}$ on $\tilde{S}$, such that the induced holomorphic flow complexes, G and $\tilde{G}$, are isomorphic. We arrange the segments of G and $\tilde{G}$ in a consistent way, such that $f \in G$ corresponds to $\tilde{f} \in \tilde{G}$. Let $\phi : G \to \tilde{G}$ be the piecewise linear map that maps the parameter domain of each f to that of $\tilde{f}$. Then we define an (asymmetric) intrinsic metric from S to $\tilde{S}$ with respect to ω and $\tilde{\omega}$ as

$$E_0(S,\tilde{S},\omega,\tilde{\omega}) = \sum_{f\in G}\int_f (\lambda(u,v) - \tilde{\lambda}\circ\phi(u,v))^2 du dv, \tag{4}$$

and similarly, the extrinsic metric as

$$E_1(S,\tilde{S},\omega,\tilde{\omega}) = \sum_{f\in G}\int_f (H(u,v) - \tilde{H}\circ\phi(u,v))^2 du dv. \tag{5}$$

Then the (symmetric) intrinsic distance between S and $\tilde{S}$ is

$$d_0(S,\tilde{S}) = \inf_{\omega,\tilde{\omega}}[E_0(S,\tilde{S},\omega,\tilde{\omega}) + E_0(\tilde{S},S,\tilde{\omega},\omega)],$$

and the extrinsic distance between S and $\tilde{S}$ is

$$d_1(S,\tilde{S}) = \inf_{\omega,\tilde{\omega}}[E_1(S,\tilde{S},\omega,\tilde{\omega}) + E_1(\tilde{S},S,\tilde{\omega},\omega)],$$

where ω and $\tilde{\omega}$ induces isomorphic holomorphic flow graphs. The intrinsic metric depends only on the Riemannian metrics and is independent of the embeddings.

6. Experimental Results. The algorithms are developed using C++ on Windows XP platform, and tested with a dual processor PC with main frequency 3.2GHz. The execution time statistics are illustrated in table 1.

TABLE 1

Execution time (unit: minute) of the parameterization and segmentation steps. The experiments are conducted on a dual processor PC (main frequency: 3.2*GHz) with Windows XP platform.*

Model	Genus #	Parameterization	Segmentation
bull	7	10.5	8.1
horse	4	8.7	6.2
tyra	6	11.2	8.2
sculpture	3	10.5	7.5

We tested our algorithms on several models acquired by laser scanning.

Figure 3 illustrate the experimental results. For the bull surface on the first row, we introduce small slices at the tips of its horns, feet, tail and mouth. Then we double cover it to get a genus 6 symmetric surface. Any global conformal surface parameterization has total 10

zero points. There are five on the outer side of the double covering. The iso-u curves through these zero points are orthogonal to the boundaries, and segment the surface to several disks. Each patch is conformally mapped to a rectangle in the last picture on the first row. The horse model and tyrannosaur model are on the second and third row in Figure 3. They are processed in the same way. Each of them are segmented using holomorphic flow. Each segment is a topological disk, and can be conformally mapped to a rectangle. The kissing sculpture (fourth row in Figure 3) model is of genus 3, there are 4 zero points. The holomorphic flow through these 4 points segment the whole surface to 6 patches, each patch is a topological cylinder.

Figure 2 illustrate three morphing experiments. The first two rows in Figure 2 shows a morphing among three surfaces, the Max Planck head (left on the first row) is morphed to a real male head (left on the second row) first, then morphed to the David head surface (right on the third row). The morphing is smooth and natural. The fourth and fith rows show a morphing between high genus surfaces. The vase model and eight model share the same topology structure although their geometry are much different. The morphing between human bodies is more complicated. The human surface has 5 boundaries. Its double covering is genus 4, there are 3 zero points on the surface, two of them are under the armpits, and one is at the bottom. The holomorphic flow segmentations are consistent through surfaces with different postures, because they share the same Riemannian metric. It can be verified that the zero point positioins, the vertical trajectories are consistent. In fact, all segments are mapped to rectangles on the parameter plane conformally, the shapes of corresponding rectangles are similar also. The morphing is illustrated in the last two rows in figure 2.

We study the distances between male head model, David head model, and Max Planck model. With three geometry images used for morphing experiment, we compute the intrinsic and extrinsic metrics with Equation 4 and Equation 5. The results are listed in Table 2. From the results, it is clear that the male head model is closer to Max Planck model than to David head model. It is consistent with our intuition since the hair on David head makes it different from the other two.

TABLE 2

Computed intrinsic and extrinsic metrics between Max-Male pair and Male-David pair. The metrics are defined in Equation 4 and Equation 5, separately.

Pair	λ distance d_0	Mean Curvature Distance d_1
Max - Male	0.109611	0.000011
Male - David	0.433798	0.000105

7. Conclusion and Future Work. This paper introduces a novel surface segmentation method, holomorphic flow segmentation. This method is based on Riemann surface theories and differential geometry. Following a global conformal parameterization, it automatically locates zero points and trace horizontal and vertical lines. This method is independent of surface embedding, intrinsic to the geometry, and works with arbitrary surface with high genus

and multiple boundaries. We further demonstrate our method by applying it to geometric morphing and surface matching problems.

In the future, we will explore the approach to compute the unique harmonic map between two surfaces which minimize the distorsion between their conformal structures based on holomorphic segmentation method. It is also interesting to generalize this segmentation method to other surface parameterization methods.

REFERENCES

[ACOL00] M. ALEXA, D. COHEN-OR, AND D. LEVIN, *As-rigid-as-possible shape interpolation*, In: SIGGRAPH 00(2000), pp. 157–164.

[AHTK99] S. ANGENENT, S. HAKER, A. TANNENAUM, AND R. KIKINIS, *Conformal geometry and brain flattening, MICCAI* (1999), 271–278.

[AMD02a] P. ALLIEZ, M. MEYER, AND M. DESBRUN, *Interactive geometry remeshing*, In: SIGGRAPH 02(2002), pp. 347–354.

[AMD02b] P. ALLIEZ, M. MEYER, AND M. DESBRUN, *Interactive geomety remeshing*, In: SIGGRAPH 02(2002), pp. 347–354.

[CDST97] B. CHAZELLE, D. DOBKIN, N. SHOURHURA, A. TAL, *Stragegies for polyhedral surface decomposition: An experimental study*, In: Computational Geometry: Theory and Applications (1997), Vol. 7, pp. 327–342.

[CP97] B. CHAZELLE AND L. PALIOS, *Decomposing the boundary of a nonconvex polytope*, Algorithmica 17:3(1997), pp. 1286–1302.

[EDD*95] M. ECK, T. DEROSE, T. DUCHAMP, H. HOPPE, M. LOUNSBERY, AND W. STUDTZLE, *Multiresolution analysis of arbitrary meshes*, In: SIGGRAPH 95(1995), pp. 173–182.

[Flo97] M. FLOATER, *Parameterization and smooth approximation of surface triangulations*, In: Computer Aided Geometric Design (1997), Vol. 14, pp. 231–250.

[Flo03] M. FLOATER, *Mean value coordinates*, In: Computer Aided Geometric Design (2003), Vol. 20, pp. 19–27.

[GSL*99] A. GREGORY, A. STATE, M. LIN, D. MANOCHA, M. LIVINGSTON, *Interactive surface decomposition for polyhedral morphing*, In: The Visual Computer (1999), Vol. 15, pp. 453–470.

[GWC*04] X. GU, Y. WANG, T. CHAN, P. THOMPSON, S.-T. YAU, *Genus zero surface conformal mapping and its application to brain surface mapping*, IEEE Transaction on Medical Imaging 23:7(2004).

[GWH01] M. GARLAND, A. WILLMOTT, AND P. HECKBERT, *Hierarchical face clustering on polygonal surfaces*, In: Proceedings of ACM Symposium on Interactive 3D Graphics (2001), pp. 49–58.

[GWY04] X. GU, Y. WANG, S.-T. YAU, *Multiresolution computation of conformal structures of surfaces*, Journal of Systemics, Cybernetics and Informatics 1:6 (2004).

[GY02] X. GU AND S. YAU, *Computing conformal structures of surfaces*, Communication of Information and Systems (December 2002).

[GY03] X. GU AND S.-T. YAU, *Global conformal surface parameterization*, In: ACM Symposium on Geometry Processing (2003), pp. 127–137.

[HAT*00a] S. HAKER, S. ANGENENT, A. TANNENBAUM, R. KIKINIS, G. SAPIRO, AND M. HALLE, *Conformal surface parameterization for texture mapping*, IEEE TVCG 6:2(2000), pp. 181–189.

[HAT*00b] S. HAKER, S. ANGENENT, A. TANNENBAUM, R. KIKINIS, G. SAPIRO, AND M. HALLE, *Conformal surface parameterization for texture mapping*, IEEE Transactions on Visualization and Computer Graphics, 6 (April-June 2000), pp. 240–251.

[HG99] K. HORMAN AND G. GREINER, *Mips: An efficient global parameterization method*, In: Curve and Surface Design: Saint-Malo 1999 (1999), Vanderbilt University Press, pp. 153–162.

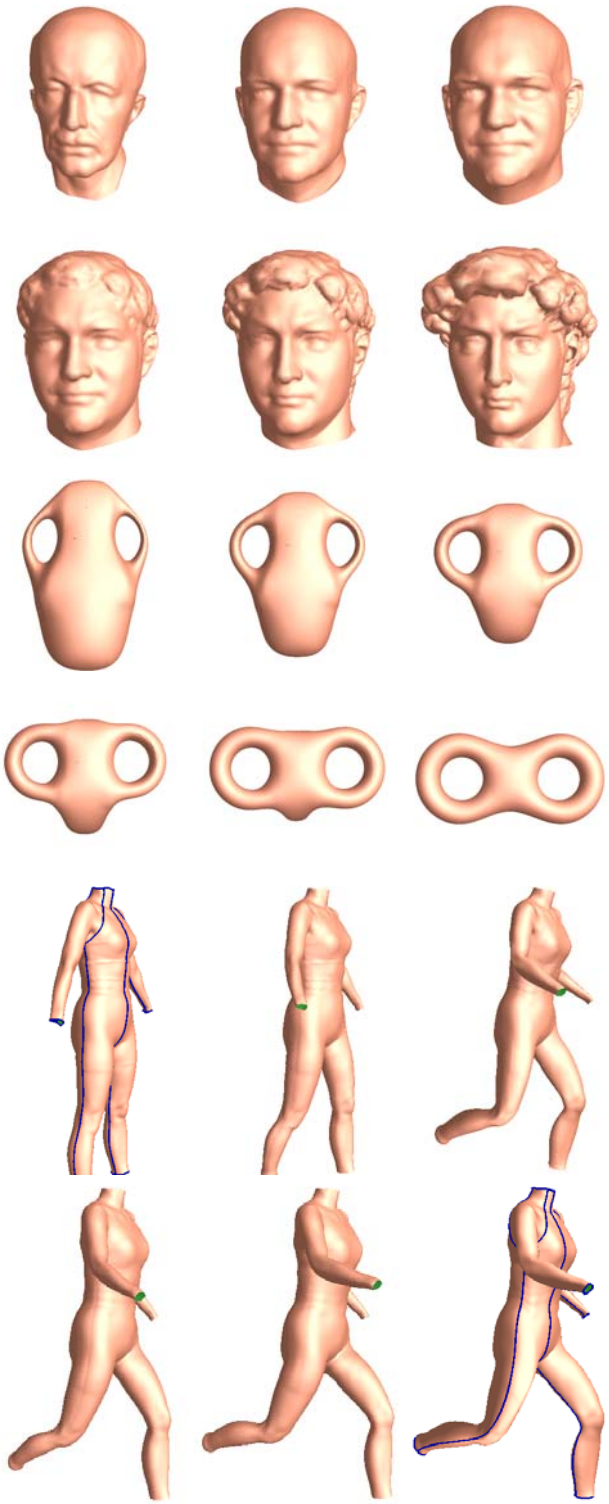

FIG. 2. *Geometric Morphing based on holomorphic flow examples. The surfaces are consistently segmented using holomorphic 1-forms, Segments are matched using constrained harmonic maps.*

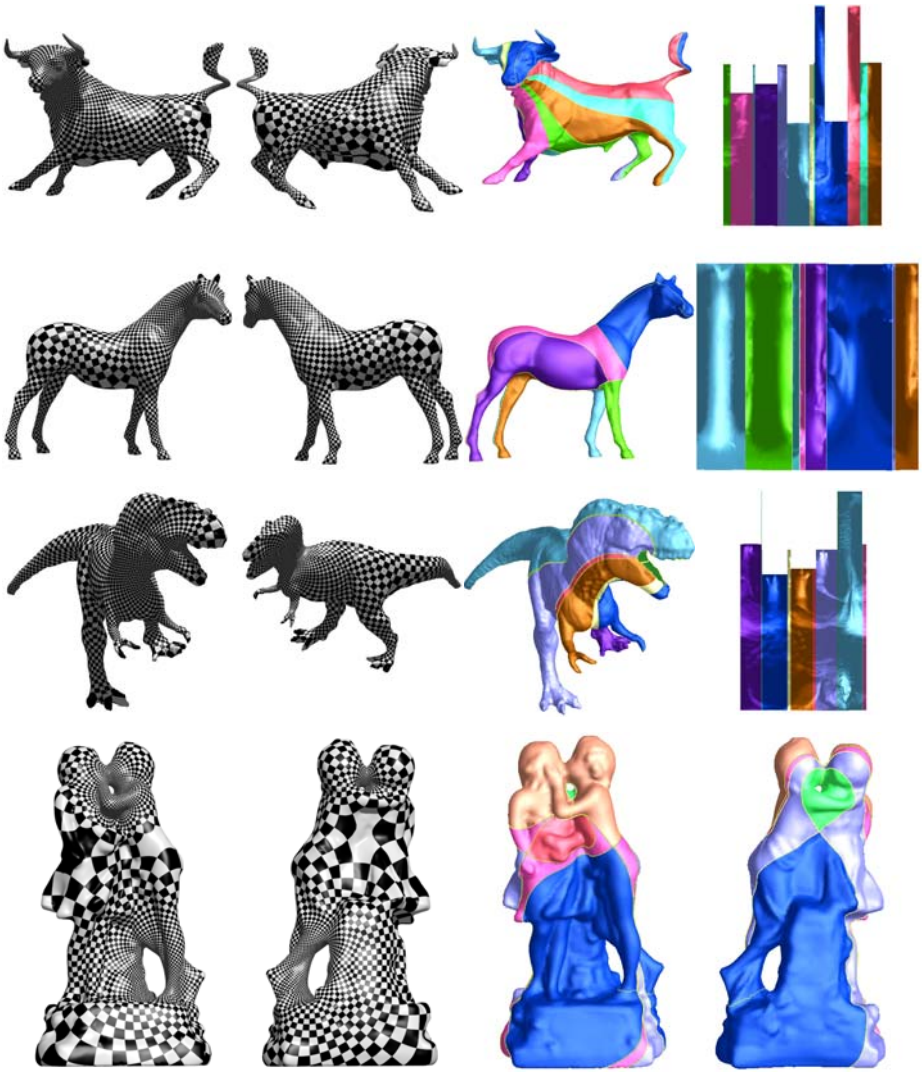

FIG. 3. *Holomorphic flow segmentation of the bull model (first row), horse model (second row), tytranosaur model (third row) and kissing sculpture model (fourth row). The segments are color encoded. The first three surfaces are topologically modified, so their double covered surfaces are symmetric, the conformal parameter domain of each segment is a rectangle. The vertical trajectories through zero points of the sculpture surface are illustrated in the last row, each segment is a topological cylinder.*

[Jos91] J. JOST, *Compact Riemann Surfaces: An Introduction to Contemporary Mathematics*, Springer, 1991.

[KSG03] V. KRAEVOY, A. SHEFFER, AND C. GOTSMAN, *Matchmaker: Constructing constrained texture maps*, In: SIGGRAPH 03 (2003), pp. 326–333.

[KT03] S. KATZ AND A. TAL, *Hierarchical mesh decomposition using fuzzy clustering and cuts*, In: SIGGRAPH 03 (2003), pp. 954–961.

[LÓ3] B. LÉVY, *Dual domain extrapolation*, In: SIGGRAPH 03 (2003), pp. 364–369.

[LPRM02] B. LEVY, S. PETITJEAN, N. RAY, AND J. MAILLOT, *Least squares conformal maps for automatic*

texture atlas generation, In: SIGGRAPH 02 (2002), pp. 362–371.

[LTTH01] X. LI, T. TOON, T. TAN, AND Z. HUANG, *Decomposing polygon meshes for interactive applications*, In: Proceedings of ACM symposium on Interactive 3D graphics (2001), pp. 35–42.

[MW99] A. MANGAN AND R. WHITAKER, *Partitioning 3d surface meshes using watershed segmentation*, IEEE Transactions on Visualization and Computer Graphics, 5:4 (1999), pp. 308–321.

[OBA*03] Y. OHTAKE, A. BELYAEV, M. ALEXA, G. TURK, H.-P. SEIDEL, *Multi-level partition of unity implicits*, In: SIGGRAPH 03 (2003), pp. 463–470.

[PH03] E. PRAUN AND H. HOPPE, *Spherical parametrization and remeshing*, In: SIGGRAPH 03 (2003), pp. 340–349.

[SM00] J. SHI AND J. MALIK, *Normalized cuts and image segmentation*, IEEE Transactions on Pattern Analysis and Machine INtelligence, 22:8(2000), pp. 888–905.

[STK02] S. SHLAFMAN, A. TAL, AND S. KATZ, *Metamorphosis of polyhedral surfaces using decomposition*, In: Eurographics (2002), pp. 219–228.